NANO LETTERS

Letter

pubs.acs.org/NanoLett

Enhancing Flow Boiling Heat Transfer in Microchannels for Thermal Management with Monolithically-Integrated Silicon Nanowires

D. Li,[†,‡,§] G. S. Wu,[†,⊥,§] W. Wang,[†] Y. D. Wang,[†] Dong Liu,[∥,*] D. C. Zhang,[‡] Y. F. Chen,[⊥] G. P. Peterson,[#] and Ronggui Yang[†,*]

[†]Department of Mechanical Engineering, University of Colorado, Boulder, Colorado 80309, United States

[‡]Department of Microelectronics, Peking University, Beijing, 100871, China

[⊥]School of Mechanical Engineering, Southeast University, Nanjing, Jiangsu, 211189, China

[∥]Department of Mechanical Engineering, University of Houston, Houston, Texas 77204, United States

[#]School of Mechanical Engineering, Georgia Institute of Technology, Atlanta, Georgia 30332, United States

Supporting Information

ABSTRACT: Thermal management has become a critical issue for high heat flux electronics and energy systems. Integrated two-phase microchannel liquid-cooling technology has been envisioned as a promising solution, but with great challenges in flow instability. In this work, silicon nanowires were synthesized *in situ* in parallel silicon microchannel arrays for the first time to suppress the flow instability and to augment flow boiling heat transfer. Significant enhancement in flow boiling heat transfer performance was demonstrated for the nanowire-coated microchannel heat sink, such as an early onset of nucleate boiling, a delayed onset of flow oscillation, suppressed oscillating amplitudes of temperature and pressure drop, and an increased heat transfer coefficient.

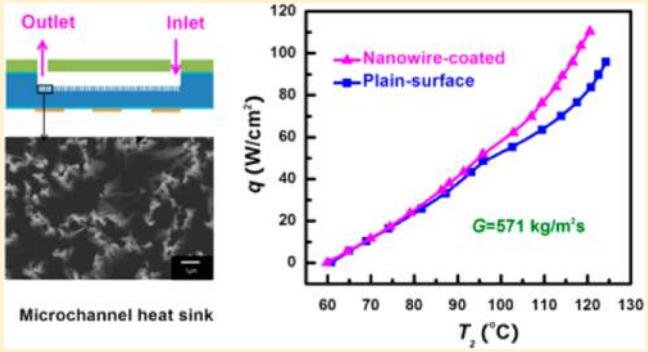

KEYWORDS: *Si nanowires, microchannels, flow boiling, thermal management*

High-flux heat dissipation is becoming the bottleneck to increasing the reliability and enhancing the energy efficiency of many high power electronics and energy systems. Among various thermal management approaches, integrated two-phase microchannel liquid-cooling technology is envisioned to be a promising solution.[1−3] Flow boiling in microchannels can significantly enhance the temperature uniformity in the device substrate along the flow direction as well as reduce the thermal resistance.[4−6] However, a major challenge that hinders the implementation of two-phase microchannel heat sinks for practical applications is the severe flow instability.[7,8] Over the past two decades, much effort has been made to improve the flow boiling heat transfer performance in microchannels.[10−12] For example, it was found that the heat transfer coefficient (HTC) can be increased by creating notches in the sidewalls of the microchannels,[13] and nearly steady flow boiling condition was realized by using inlet flow restrictors.[14] More recently, microsized artificial nucleation sites, including micro pin fins[15,16] and reentrant cavities,[17] have been integrated into microchannels, and the heat transfer improvements have been demonstrated. These structured surfaces can mitigate the flow boiling instability induced by the rapid bubble growth at random locations in the microchannels. However, the number and size distribution of the artificial nucleation sites are limited by the microfabrication technology used for fabricating these devices.

Very recently, Chen et al.[18] and Li et al.[19] showed that nanowires can significantly enhance the pool boiling heat transfer performance. It was found that the nanowire-coated surfaces are superhydrophilic, and the agglomeration of the nanowires gives rise to numerous nucleation cavities with sizes ranging from submicrometer to a few micrometers, which help enhance HTC and delay CHF of pool boiling. Following the same line of reasoning, we expect that the nanowire coatings could similarly enhance the flow boiling performance of microchannel heat sinks if the nanowires can be successfully integrated in microchannels.

In this work, we study the effect of nanowires on the flow boiling heat transfer in a two-phase microchannel heat sink. We present for the first time the fabrication of parallel microchannel arrasy with *in situ* silicon nanowire integration. By comparing the flow boiling characteristics in microchannels with and without nanowires, we demonstrate that the flow boiling performance can be significantly enhanced in the nanowire-coated microchannels with an early onset of nucleate

Received: January 5, 2012
Revised: May 15, 2012
Published: June 13, 2012

   dx.doi.org/10.1021/nl300049f | *Nano Lett.* 2012, 12, 3385−3390

boiling (ONB), a delayed onset of flow oscillation (OFO), suppressed oscillating amplitude of temperature and pressure drop, and an augmented HTC.

We fabricated both the plain-surface microchannel arrays and the nanowire-coated microchannel arrays. Figure 1 shows the

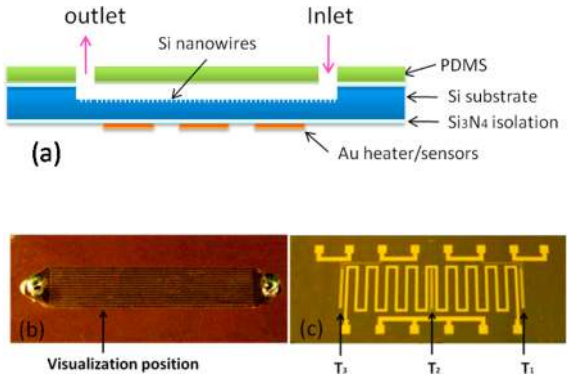

Figure 1. (a) Schematics of the nanowire-coated microchannels and the optical images of the microfabricated device: (b) Top view from the transparent PDMS cap and (c) backside view with gold thin film heater and resistive temperature sensors.

schematics of the Si nanowire-coated microchannels (a) and the photos of the actual fabricated device (b, c). Both the plain-surface and the nanowire-coated microchannel arrays consist of 14 parallel channels with inlet/outlet plenums, the PDMS cap, and the on-chip heating element and temperature sensors. Each microchannel is 20 mm long, 250 μm wide, and 200 μm deep. The microchannels are equally spaced with a channel wall thickness of 90 μm. The footprint of the microchannel array is 20 mm ×4.67 mm on the silicon substrate, and at the backside a gold thin film heater of the same size is fabricated to provide electrical resistive heating. Three resistance temperature sensors (also made of gold) are fabricated on the heater side to measure the temperatures at the inlet, the outlet and the middle location of the microchannels, T_1, T_2, and T_3, respectively. Figure 2

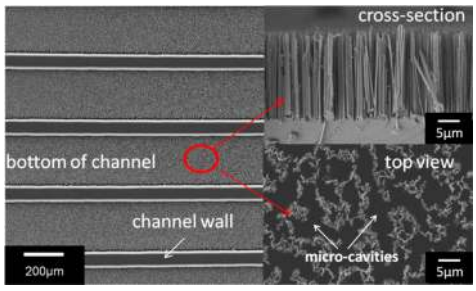

Figure 2. SEM images of the Si nanowire-coated microchannels before flow boiling tests. On the right are the cross-sectional and the top views of the nanowire arrays on the microchannel surface. Due to the agglomeration of the nanowires, numerous microcavities with a size range of a few micrometers are formed, which could serve as the boiling nucleation sites.

shows the scanning electron microscopy (SEM) images of the top view and the cross-sectional view of the Si nanowire arrays in the microchannels before flow boiling experiments. It is observed that Si nanowires are vertical to the substrate and numerous microcavities are formed due to the entanglement of these high aspect-ratio nanowires during the fabrication process. The detailed fabrication processes are described in Supporting Information (Figure S1).

Using the similar testing procedure as reported by Liu and Garimella,[20] we tested the flow boiling characteristics of both the plain-surface microchannels and the nanowire-coated microchannels at different mass fluxes. Schematics of the test setup and the experimental procedure, together with the data reduction and measurement uncertainty, are reported in Supporting Information (Figures S2 and S3). Generally, it was found that at low heat fluxes the wall temperature increases linearly with the heat flux, which indicates the flow is in the single-phase liquid flow regime. With increasing heat flux, vapor bubbles start to form in the microchannels, and the ONB is identified by visual inspection of the first appearance of the vapor bubbles. Following ONB, further increase in the heat flux results in periodic temperature and pressure fluctuations with considerable amplitude. This condition is identified as the OFO, where the vapor phase generated may even surge upstream against the incoming liquid. If we continue to increase the heat flux to a sufficiently high level, a rapid and unsteady temperature rise will be observed at the exit of the microchannels (corresponding to the location of temperature sensor T_3). The temperature rise is accompanied by a fast vapor backflow toward the inlet, which could completely block the liquid supply into the microchannel and result in device failure due to overheating. In our experiments, this is recognized as the CHF condition.

Figure 3 compares the flow boiling curves for both the plain-surface microchannels and the nanowire-coated microchannels, where the inlet fluid temperature T_{in} is fixed at 60 °C and the mass flux G varies from 119 to 571 kg/m^2 s. It is noted that because of the axial conduction effect on the wall temperature measurements, T_2 which is measured at the middle location of the microchannel array (as shown in Figure 1c) is taken as the representative wall temperature. Additional flow boiling curves for T_{in} = 30 °C at mass fluxes G = 119−571 kg/m^2 s can be found in Supporting Information (Figure S5). An early ONB at a lower heat flux is observed in Figure 3 for the nanowire-coated microchannels as compared with that for the plain-surface microchannels. After ONB, a rapid transition to OFO occurs in the plain-surface microchannels, accompanied by periodical temperature and pressure fluctuations. This is due to the rapid bubble growth following ONB at random locations in the microchannels, which limits the heat flux range for stable flow boiling. In contrast, stable flow boiling is observed in the nanowire-coated microchannels over a much larger range of heat flux. Thus, flow instability is suppressed in the nanowire-coated microchannels. Additionally, once the mass flux reaches 238 kg/m^2 s and above, appreciable heat transfer enhancement can be found in the nanowire-coated microchannels, as evidenced by the reduced wall temperature when comparing with that in the plain-surface microchannels (Figure 3, parts b−d).

The time-dependence of the wall temperature T_2 is illustrated in Figure 4a for G = 571 kg/m^2 s and q = 80 W/cm^2. In the nanowire-coated microchannels, the average wall temperature is about 8 °C lower than that in the plain-surface microchannels, and the amplitude of temperature fluctuations also decreases significantly. According to Kandlikar,[21] reduction of the wall temperature is one effective way to suppress flow instability. Figure 4b shows the pressure drop across the microchannels under the same flow conditions. Similarly, the average pressure drop in the nanowire-coated microchannels is

dx.doi.org/10.1021/nl300049f | Nano Lett. 2012, 12, 3385−3390

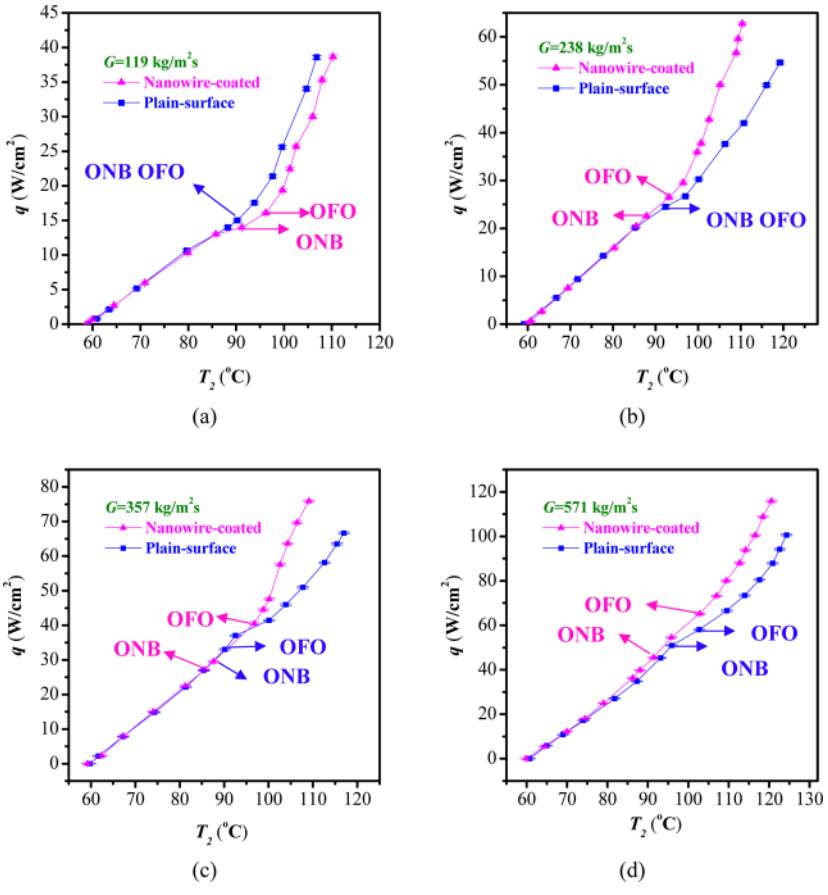

Figure 3. Flow-boiling curves for the plain-surface microchannels and the nanowire-coated microchannels for mass fluxes ranging from G = 119 to G = 571 kg/m^2 s. Tests are conducted at T_{in} = 60 °C. (Note that error bars are too small to be shown in the figure.)

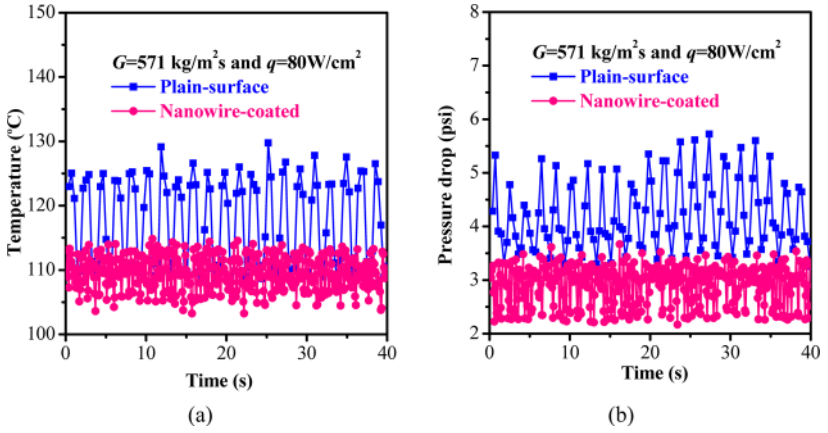

Figure 4. The oscillation of the temperature in the middle section of the array (T_2) and the oscillation of the pressure drop for both the plain-surface microchannels and the nanowire-coated microchannels at a heat flux q = 80 W/cm^2 when the mass flux is G = 571 kg/m^2 s. Tests are conducted at T_{in} = 60 °C.

decreased by 1.1 psi and the fluctuations are decreased by 1 psi as compared to those in the plain-surface microchannels. Thus, Figure 4 demonstrates that the nanowire coatings indeed help suppress the flow instability in the microchannels.

To understand the heat transfer enhancement mechanisms, we visualized the flow boiling characteristics using a high-speed camera (FASTCAM SA4). Figure 5 shows the two-phase flow patterns in the middle channel of the microchannel array for G = 357 kg/m^2 s and q = 48 W/cm^2. The images presented were taken at a location 6 mm downstream to the inlet. The moderate values of mass flux and heat flux were chosen because they produce well-defined flow patterns. The flow patterns in the nanowire-coated microchannels are less distinguishable than those in the plain-surface microchannels, due to the light absorption by the nanowires.[22] Hence the outlines of the flow patterns are sketched in Figure 5 to facilitate the comparison. While Figure 5 only shows the static images, periodic two-phase flow motions were observed when the heat flux increases beyond the OFO, and one cycle can be divided into three

dx.doi.org/10.1021/nl300049f | Nano Lett. 2012, 12, 3385−3390

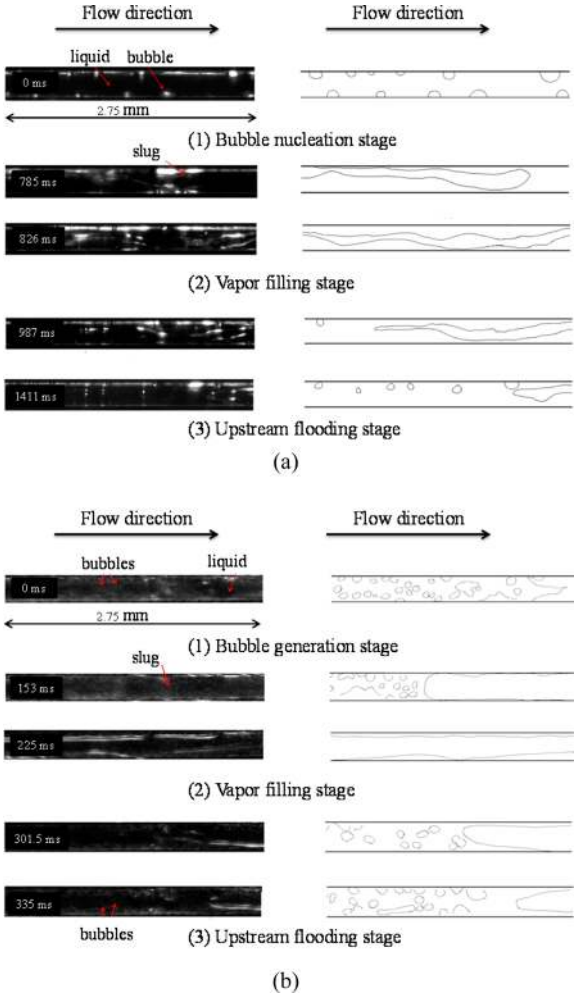

Figure 5. Transient flow patterns in (a) a plain-surface microchannel and (b) a nanowire-coated microchannel. Tests are conducted at T_{in} = 60 °C, with mass flux G = 357 kg/m^2 s and heat flux q = 48 W/cm^2.

stages: the bubble nucleation stage, the vapor filling stage, and the upstream flooding stage.

(1) During the bubble nucleation stage, sparse vapor bubbles appears primarily at the corner of the plain−surface microchannel where the highest wall superheat is reached (Figure 5a). In contrast, more abundant bubbles are found uniformly distributed in the nanowire-coated microchannel (Figure 5b). The flow boiling enhancement by the nanowire coatings[18,19] can be explained as following. First, while the nanowire-coated surface exhibits superhydrophilicity with a contact angle of 6° for water (see Figure S6 in Supporting Information), the agglomeration of nanowires gives rise to numerous micrometer-sized cavities ranging from 1 to 15 μm (as shown in Figure 2). These cavities provide ample active nucleation sites that contribute to the early ONB and the enhanced HTC[23] (refer to Figure S7, Supporting Information). Second, the nanowires also serve as nanoscale pin fins that dramatically increase the effective heat transfer area for heat conduction from the microchannel surface into the liquid flow.

(2) During the vapor filling stage in the plain-surface microchannels, the coalescence of bubbles merely creates an elongated vapor thread due to insufficient vapor production from the bubble nucleation stage (Figure 5a). The vapor thread meanders through the channel, causing large oscillations in both the temperature and pressure fields as shown in Figure 4. In the nanowire-coated microchannels, the large amount of vapor bubbles generated earlier quickly coalesce into vapor slugs congesting the channel and, in the meanwhile, the vapor phase velocity increases because of the increased local vapor quality. Consequently, annular flow pattern is formed easily where the vapor phase flows through a central core and the liquid phase is confined in a thin film flowing around the channel wall (Figure 5b). Since the annular flow induces much lower flow fluctuations compared to other flow patterns such as the bubbly flow and slug flow,[24] the formation of annular flow pattern in the nanowire-coated microchannels helps to suppress the temperature and pressure fluctuations associated with the two-phase flow instability.

(3) During the upstream flooding stage, the pressure is built up at upstream location, as the channels are congested by the vapor phase, to a certain point that it pushes the single-phase liquid to flow downstream in both the plain-surface microchannels and the nanowire-coated microchannels, which flushes away the intermittent flow patterns and causes the wall temperature and pressure drop to decrease.

To quantify the flow boiling performance, the boiling heat transfer coefficients are calculated for both the plain-surface microchannels and nanowire-coated microchannels (see Section S3 in Supporting Information). Figure 6 shows a decreasing trend in the boiling heat transfer coefficient as a function of the wall superheat, which is a typical feature for annular flow heat transfer in microchannels.[4,5] It is also seen that the heat transfer coefficient is enhanced in nanowire-coated microchannels at higher mass fluxes, i.e., G = 238, 357, and 571 kg/m^2 s; however, at the lowest mass flux of G = 119 kg/m^2 s, the boiling heat transfer becomes inferior to that in the plain-surface microchannels. This can be explained by the evolution of the annular flow pattern at different mass fluxes in the nanowire-coated microchannels (see detailed discussion in Section S7 of Supporting Information). Annular flow is beneficial to boiling heat transfer due to the transient heat transfer conduction and strong interfacial evaporation through the thin liquid film, however, it is also prone to local dryout if the liquid film vanishes, for instance, when there is insufficient liquid to replenish the evaporated mass, depending on the heat-to-mass flux ratio, q/G. At higher mass flux, the liquid film forms more easily and is able to persist through the duration of annular flow in the nanowire-coated microchannels (shown in Figure 5(b)), which results in enhanced boiling heat transfer. But at the lowest mass flux, the liquid film disappears more quickly in the two-phase flow cycle in the nanowire-coated microchannels (shown in Figure S8), and the consequent dryout leads to inferior heat transfer performance comparing to that in the plain-surface microchannels.

To examine the structural integrity, we have carefully inspected the nanowire-coated microchannels after the flow boiling test at q = 115 W/cm^2 for the highest mass flux of G = 571 kg/m^2 s. As shown in Figure 7, no visible morphology change can be detected for the nanowire coatings, and the microcavities remain almost identical to those before the test (as shown in Figure 2). Therefore, due to the native bounding

dx.doi.org/10.1021/nl300049f | Nano Lett. 2012, 12, 3385−3390

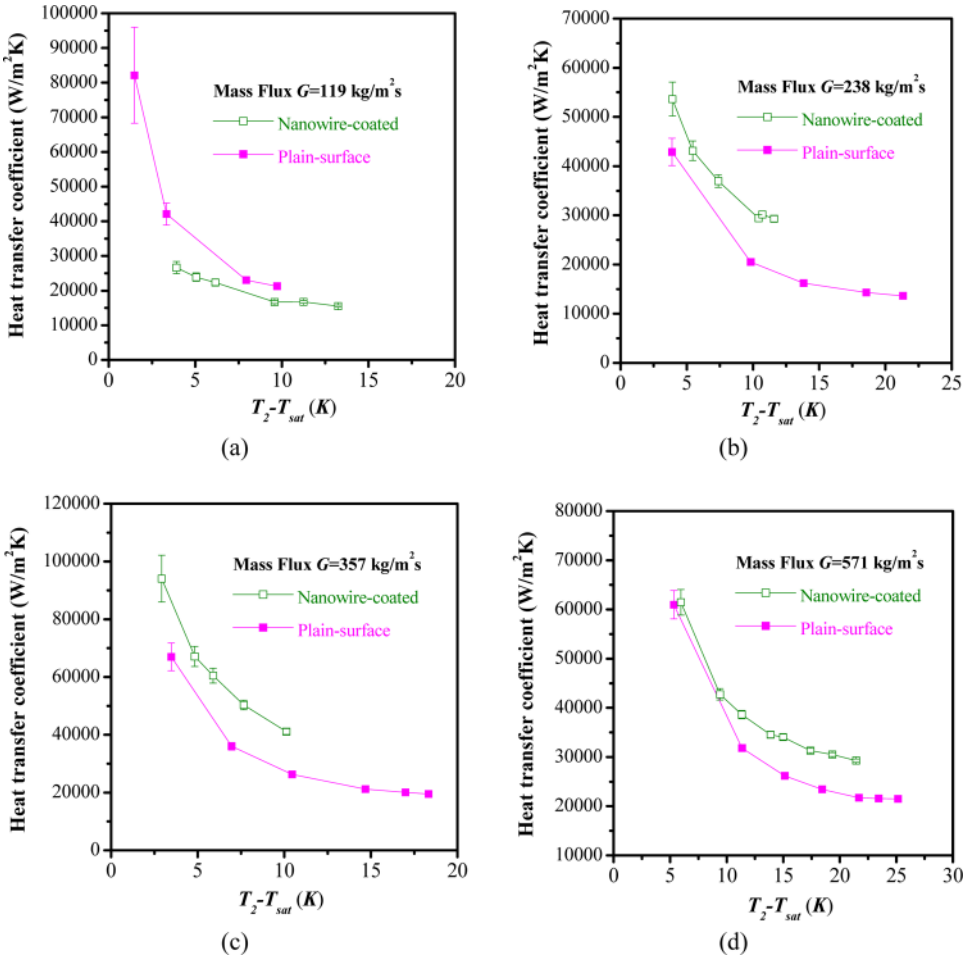

Figure 6. Heat transfer coefficients for the plain-surface microchannels and the nanowire-coated microchannels for mass fluxes ranging from G = 119 kg/m^2 s to G = 571 kg/m^2 s. (Note that some error bars are too small in the scale to be shown in the figure.)

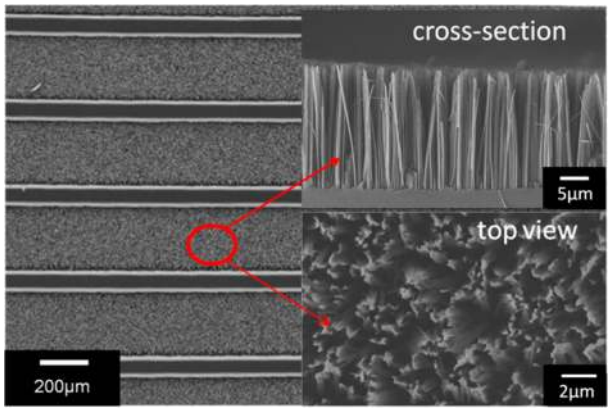

Figure 7. SEM images of the Si nanowire-coated microchannels after flow boiling tests. On the right are the cross-sectional and the top views of the nanowire arrays on the microchannel surface. Stable Si nanowire coatings could enable long-term flow boiling performance enhancement.

between the nanowires and the Si substrate, the nanowire coatings are robust and can be used to enhance the flow boiling heat transfer performance over a long period of time.

In summary, we present in this Letter the very first effort on exploiting the integration of nanowires in microchannel heat sinks for enhancing flow boiling heat transfer. A monolithic micro/nanofabrication process has been developed to fabricate silicon nanowire-coated microchannels. Flow boiling heat transfer tests were conducted in both the plain-surface microchannels and the nanowire-coated microchannels. The wall temperature and pressure drop measurements were taken over a wide range of mass flux and applied heat flux, and the two-phase flow patterns were visualized. It is found that flow boiling heat transfer is significantly enhanced in the nanowire-coated microchannels, including an early onset of nucleate boiling, a delayed onset of flow oscillation, suppressed oscillating amplitude of temperature and pressure drop, and an augmented heat transfer coefficient at moderate-to-high mass flux. The enhancement is attributed to abundant nucleation sites with a wide size range, enhanced capillary wetting facilitated by the superhydrophilic surface as well as the promoted formation of annular flow pattern. At low mass flux, the flow boiling performance is degraded in the nanowire-coated microchannels due to early dryout of the liquid film in the annular flow. Finally, the nanowire coatings are found to be very stable, due to the native bounding between the nanowires and Si substrate, and can enable long-term flow boiling performance enhancement.

■ ASSOCIATED CONTENT

Ⓢ Supporting Information

The fabrication processes of the microchannel arrays, experimental details about data reduction, contact angle

dx.doi.org/10.1021/nl300049f | Nano Lett. 2012, 12, 3385−3390

measurement, plot of active size range of nucleate boiling, and supplementary results and high-speed images. This material is available free of charge via the Internet at http://pubs.acs.org.

AUTHOR INFORMATION

Corresponding Author

*(D.L.) Telephone: 713-743-4532. E-mail: dongliu@uh.edu. (R.Y.) Telephone: 303-735-1003. Fax: 303-492-3498. E-mail: ronggui.yang@colorado.edu.

Author Contributions

§These authors contributed equally to this work

Notes

The authors declare no competing financial interest.

ACKNOWLEDGMENTS

This work was supported by the DARPA Thermal Ground Plane Program managed by Dr. Thomas W. Kenny and Dr. Avram Bar-Cohen (N66001-08-C-2006). The microfabrication process described in this work was conducted in the Colorado Nanofabrication Laboratories, which is supported by the NNIN and the National Science Foundation under Grant No. ECS-0335765. The views expressed are those of the author and do not reflect the official policy or position of the Department of Defense or the U.S. Government. D.L. and G.S.W. would like to express thanks for the financial support from the China Scholarship Council.

REFERENCES

(1) Greiner, M.; Chen, R.-F.; Wirtz, R. A. *J. Heat Transfer* **1989**, *112*, 336−341.
(2) Berglesa, A. E.; Lienhard V, J. H.; Kendalla, G. E.; Griffitha, P. *Heat Transfer Eng.* **2003**, *23*, 18−40.
(3) Thome, J. R. *Int. J. Heat Fluid Flow* **2004**, *25*, 128−139.
(4) Qu, W.; Mudawar, I. *Int. J. Heat Mass Transfer* **2003**, *46*, 2755−2771.
(5) Qu, W.; Mudawar, I. *Int. J. Heat Mass Transfer* **2003**, *46*, 2773−2784.
(6) Zhang, L.; Wang, E. N.; Goodson, K. E.; Kenny, T. W. *Int. J. Heat Mass Transfer* **2005**, *48*, 1572−1582.
(7) Yuncu, H.; Yildirim, O. T.; Kakac, S. *Appl. Sci. Res.* **1991**, *48*, 83−104.
(8) Zhang, L.; Koo, J. M.; Jiang, L.; Asheghi, M.; Goodson, K. E.; Santiago, J. G.; Kenny, T. W. *J. Microelectromech. Syst.* **2002**, *11*, 12−19.
(9) Kuo, C. J.; Peles, Y. *J. Heat Transfer* **2008**, *130*, 072403−1.
(10) Liu, D.; Garimella, S. V. *J. Heat Transfer* **2007**, *129*, 1321−1332.
(11) Zhang, T. J.; Tong, T.; Chang, J.-Y.; Peles, Y.; Prasher, R.; Jensen, M. K.; Wen, J. T.; Phelan, P. *Int. J. Heat Mass Transfer* **2009**, *52*, 5661−5674.
(12) Zhang, T. J.; Peles, Y.; Wen, J. T.; Tong, T.; Chang, J.-Y.; Prasher, R.; Jensen, M. K. *Int. J. Heat Mass Transfer* **2010**, *53*, 2347−2360.
(13) Zhang, L.; Wang, E. N.; Koo, J. M.; Jiang, L.; Goodson, K. E.; Santiago, J. G.; Kenny, T. W. *Proc. IEEE Micro. Elect.* **2002**, 89−92.
(14) Kosar, A.; Kuo, C. J.; Peles, Y. *J. Heat Transfer* **2006**, *128*, 251−260.
(15) Krishnamurthy, S.; Peles, Y. *Int. J. Heat Mass Transfer* **2008**, *51*, 1349−1364.
(16) Kosar, A.; Peles, Y. *Int. J. Heat Mass Transfer* **2007**, *50*, 1018−1034.
(17) Kuo, C. J.; Peles, Y. *J. Heat Transfer* **2008**, *130*, 072402−10.
(18) Chen, R.; Lu, M.-C.; Srinivasan, V.; Wang, Z.; Cho, H. H.; Majumdar, A. *Nano Lett.* **2009**, *9*, 548−553.
(19) Li, C.; Wang, Z.; Wang, P.-I.; Peles, Y.; Koratkar, N.; Peterson, G. P. *Small* **2008**, *4*, 1084−1088.
(20) Liu, D.; Garimella, S. V. *Thermal Transport in Microchannels: Single-Phase and Two-Phase Fluid Flow and Heat Transfer*; VDM Verlag: Saarbrücken, Germany, 2009.
(21) Kandlikar, S. G. *Exp. Therm. Fluid Sci.* **2006**, *30*, 441−447.
(22) Peng, K.; Xu, Y.; et al. *Small* **2005**, *11*, 1062−1067.
(23) Carey, V. P. *Liquid-Vapor Phase-Change Phenomena*; Hemisphere: Washington, DC, 1992.
(24) Liu, D.; Ning, O. *J. Therm. Sci.* **1992**, *1*, 196−202.